HHS Public Access

Author manuscript

Biochemistry. Author manuscript; available in PMC 2018 July 10.

Published in final edited form as:

Biochemistry. 2018 July 10; 57(27): 3995–4004. doi:10.1021/acs.biochem.8b00122.

Tissue-like neural probes for understanding and modulating the brain

Guosong Hong[1], **Robert D. Viveros**[2], **Theodore J. Zwang**[1], **Xiao Yang**[1], and **Charles M. Lieber**[1,2,*]

[1]Department of Chemistry and Chemical Biology, Harvard University, Cambridge, Massachusetts 02138, USA

[2]John A. Paulson School of Engineering and Applied Sciences, Harvard University, Cambridge, Massachusetts 02138, USA

Abstract

Electrophysiology tools have contributed substantially to understanding brain function, yet the capabilities of conventional electrophysiology probes have remained limited in key ways due to large structural and mechanical mismatches with respect to neural tissue. In this Perspective, we discuss how the general goal of probe design in biochemistry – that the probe or label has a minimal impact on the properties and function of the system being studied – can be realized by minimizing structural, mechanical and topological differences between neural probes and brain tissue, thus leading to a new paradigm of tissue-like mesh electronics. The unique properties and capabilities of the tissue-like mesh electronics as well as future opportunities are summarized. First, we discuss the design of an ultra-flexible and open mesh structure of electronics that is tissue-like and can be delivered in the brain via minimally-invasive syringe injection like molecular and macromolecular pharmaceuticals. Second, we describe the unprecedented tissue healing without chronic immune response that leads to seamless three-dimensional integration with a natural distribution of neurons and other key cells through these tissue-like probes. These unique characteristics lead to unmatched stable long-term, multiplexed mapping and modulation of neural circuits at the single-neuron level on a year timescale. Last, we offer insights on several exciting future directions for the tissue-like electronics paradigm that capitalize on their unique properties to explore biochemical interactions and signaling in a ‘natural’ brain environment.

TOC image

*Corresponding author: Lieber, Charles M (cml@cmliris.harvard.edu).

Notes

The authors declare no competing financial interest.

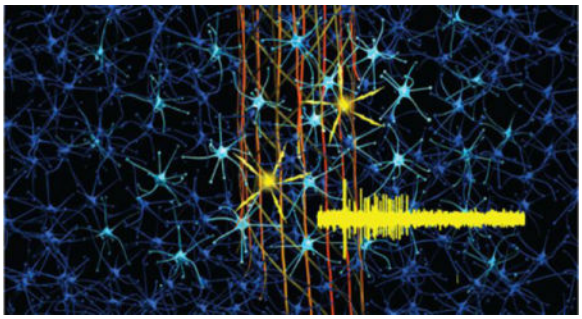

INTRODUCTION

Tools that can provide spatially resolved, real-time, and quantitative measures of the electrical activity of neurons are crucial to understanding the brain.[1] Since a capillary electrometer by Adrian[2] and a cathode ray oscilloscope by Erlanger and Gasser[3] were used for recording electrical signals conducted by nerve fibers, scientists have strived to develop tools that can improve the understanding of both the basic electrophysiology of single neurons and the functional connectivity of many neurons in the entire brain.[4,5] Despite advancements over the past century, there have remained substantial limitations of electrophysiology probes due to their fundamental structural, mechanical and topological differences with respect to neural tissue they are designed to interrogate; that is, these differences cause conventional probes to disrupt the natural properties and function of system being studied. Recognizing this issue, one can ask what are the structural, mechanical, topological, and ultimately biochemical properties that would define an ideal electrophysiology probe.

From a structural perspective, the brain features a large variety of components with sizes ranging from tens of nanometers for synapses that connect individual neurons, to tens of centimeters for long-range projections that connect distinct brain regions.[1] In comparison, silicon microelectrode arrays have overall probe sizes that are always >4 times larger than a single neuron,[6,7] although subcellular-sized recording electrodes with high density and multiplexity can be achieved by top-down fabrication processes.[8] On the other hand, microwire-based brain probes become significantly larger than neuron somata with increasing channel number,[9] despite subcellular feature size for single-channel carbon electrodes.[10,11] The relatively large size of probes may disrupt the natural three-dimensional (3D) neural connectivity and activity of relatively dense neural tissue comprising interconnected neurons, glial cells and blood vessels at the implanted site, and lead to unfavorable chronic immune response.

From a mechanical perspective, conventional brain probes also differ significantly from brain tissue. Brain tissue is extremely soft, with a small Young's modulus of 0.1-16 kPa and a bending stiffness of 10^{-4}-10^{-1} nN·m per unit width for a 20~100 μm thick brain slice.[12,13] In striking contrast, the bending stiffness values for typical 15-μm thick Si probes, ~10^5 nN·m,[14,15] single-channel carbon electrodes with diameters less than 10 μm, ~10^4 nN·m,[10,15] and typical 'flexible' probes fabricated on 10-20 μm thick bendable polyimide substrates, 10^3~10^4 nN·m,[16] are at least 100,000 to 1,000,000 times stiffer than the tissue

they are designed to interrogate. The high rigidity of these common probes is primarily due to the large Young's moduli, which describes the inability of materials to deform, and thickness of the materials used in their construction. Importantly, this large mismatch in bending stiffness leads to relative shear motion between brain tissue and the neural probes, and evokes a chronic immune response that produces glial scar formation and neuron depletion at probe-brain interfaces.[17] The near universal chronic immune response is believed to be the main contributor to reported degradation of recording and stimulation capabilities over extended time periods with common probes.[18]

From a topological perspective, the brain is comprised of highly organized and interconnected 3D networks of neurons and non-neuronal cells, such as astrocytes and microglia, that brain probes should ideally leave intact. There are several characteristics of probe design one should consider to accomplish this. On a local scale, inspired by the high degree of interpenetration between the networks of neurons and glial cells in 3D,[19] the probe should be designed to afford a similar degree of interpenetration between the implanted electronic network and the endogenous neuronal and glial networks by leaving sufficient open space for interpenetration to occur in a 3D topology. On a global scale, recognizing the cooperative importance of glial cells in defining the functional connectivity and evolution of neuronal networks in the brain,[20,21] the probe design should ensure the absence or at worst a minimal disturbance of the endogenous distribution of neurons and other cells. Despite these design principles of an ideal neural probe, conventional probes necessarily exclude a solid volume of neural tissue permanently, thus not only prohibiting 3D interpenetration with the neuronal and glial networks, but also disrupting the endogenous distribution of cells[17] and 3D diffusion of important molecular and macromolecular signaling species.[22]

As a consequence of the aforementioned structural, mechanical and topological mismatches between neural tissue and the electronic probes designed to study the neural tissue, conventional implantable brain probes adversely impact the properties and function of the neural systems being studied, and are thus generally incapable of achieving a chronically stable interface with the endogenous neural network and affording consistent long-term monitoring and modulation of brain activity at the single-neuron level.[23–28] Thus, we have focused on fundamentally new probe concepts that overcome these limitations by eliminating the distinction between the neural and electronic systems with 'tissue-like' neural probes.[15,29–35]

MESH ELECTRONICS IS DESIGNED TO MIMIC NEURAL TISSUE

Early on we began to focus this goal merging electronic and neural systems by developing subcellular-sized nanowire field-effect transistor (FET) detectors,[36–38] and porous 3D flexible device arrays.[39,40] The small sizes of nanowire FETs without loss of measurement sensitivity have allowed them to probe cells in a highly localized manner,[41,42] allowing the formation of artificial synapses with neurites[37] and minimally-invasive intracellular recording.[38,43] Incorporation of addressable nanoelectronic devices into a 3D tissue scaffold (macroporous nanoelectronic scaffold) followed by cell seeding and culture also led to the demonstration of electronically-innervated synthetic neural and cardiac tissues, where bidirectional flow of electrical and chemical signals between interpenetrated cellular and

electronic networks allows simultaneous monitoring and modulation of network activity.[40,44]

The macroporous nanoelectronic scaffold concept for synthetic or engineered tissues placed us tantalizingly close to goal of seamless 3D integration of electronic recording and stimulation devices within the brain. In particular, the macroporous nanoelectronics scaffold provided a framework now generalized to an open mesh electronics platform[40,44] where it is possible to design and realize neural probes that have (1) structural features of functional devices, conductive interconnects and support elements in the nanometer to micrometer size scale similar to that of cells in neural tissue, (2) mechanical properties on par with those of the endogenous neural tissue, and critically, (3) macroporous 3D interconnected structures that allow interpenetration of neurons and other cells without altering their endogenous distribution, as well as diffusion of key signaling molecules in the local milieu.[29]

The free-standing mesh electronics[15,29,33] (Figure 1A, I) consists of an array of recording and/or stimulation electrodes with their positions photolithographically defined at one end to target one or more brain regions (green dots in the solid black box). These electrodes are individually connected to input/output (I/O) pads at the other end of the mesh (red dots) via polymer-passivated metal interconnect wires (red lines in the dashed black box), allowing the electrodes to transmit electrical signals to and receive modulation signals from external recording and stimulation instrumentations, respectively. Structurally, the mesh electronics is designed to have the widths of longitudinal (long axis) and transverse (short axis) elements smaller than cell soma. In addition, these longitudinal and transverse elements have submicron thicknesses, and unit openings in the mesh are generally at least two orders of magnitude larger than the soma. Together these structural features result in an extremely small bending stiffness of the mesh electronics, 10^{-2}-10^{-1} nN·m, similar to that of brain tissue (10^{-4}-10^{-1} nN·m).[32] The unique structural, mechanical and topological properties of the mesh electronics not only address and overcome the key limitations of previous electrophysiological probes used for understanding and modulating the brain, but also set the stage for much more sophisticated biochemical modifications and functionalization of mesh surface, which is composed of biocompatible poly(alkylene-arylene oxide) polymer, as will be discussed in the ‘Future Directions and Outlook’ section below.

UNIQUE DELIVERY OF MESH ELECTRONICS

As a result of the unique structural, mechanical and topological design of mesh electronics, the ultra-flexible, submicron-thick mesh structures can be suspended in an aqueous solution much like colloids with apparent light scattering (Figure 1A, II).[15,34] At first glance, this characteristic and unique flexibility of the mesh raises a conundrum for minimally-invasive delivery to the brain. Conventional silicon, microwire and polymer neural probes, which have bending stiffness values significantly larger than brain tissue, can be directly inserted into the brain at the cost of long-term inflammatory immune response and chronic recording instability.[23–28] In contrast, a similar direct insertion of the tissue-like mesh electronics is not possible, and placing the mesh probe in a surgical incision would be invasive and cause local trauma. Thinking out of the box, the ultra-flexibility of mesh electronics opens up a simple yet effective solution commonly used in biology and medicine for delivery of species

ranging in size from biomolecules to viruses and cells – direct syringe injection through a needle.

A single mesh electronics probe suspended in an aqueous solution can be drawn and loaded into a syringe needle, such as a glass capillary, and then injected under positive pressure into virtually any brain region or other soft tissue in the body like pharmaceuticals and biologics with minimal invasiveness. The first demonstration of the injectable mesh electronics concept by Liu et al. in 2015 showed that centimeter-scale macroporous mesh electronics could be injected through needles with inner diameters <100 μm (Figure 1A, III) without damage to the mesh electronics.[15] During injection into a cavity, solution or body fluid the mesh electronics unrolls and expands from the point of the needle constriction, although it maintains a roughly cylindrical structure when injected into dense tissue. This initial work also led to an indication of the special chronic stability of the mesh electronics injected into neural tissue, but it was limited in terms of the ability to target precisely different brain regions. For example, because the mesh electronics is so flexible it was subject to crumpling during injection, yielding poorly defined sensor device positions with respect to specific regions within the brain. Specifically, the small size of key subfields and layers of a mouse brain requires precise injection of the mesh probe to ensure targeted delivery to a desired region: for example, the CA1 subfield of the hippocampus is ca. 620 μm thick, CA3 subfield is ca. 230 μm thick,[45] cortical layer V is ca. 300 μm thick,[46] and the dentate gyrus granular cell layer is ca. 60 μm thick.[47]

Hong et al. solved this key challenge by developing a semi-automated controlled injection method in which the rates of mesh electronics injection and needle withdrawal are balanced using a standard stereotaxic surgery stage with addition of a motorized translator and charge-coupled device (CCD)-imager (Figure 1B, I).[34] The balanced mesh injection/needle retraction is achieved by real-time optical tracking of the upper I/O pads of the mesh electronics, which are always outside of the skull, in the field of view (FoV) of the CCD (red arrow, Figure 1B, I). In this manner, it is ensured that the mesh position remains stationary in the FoV during injection by the syringe pump (green arrow, Figure 1B, I) while the needle is moved upward by a computer-controlled linear translation stage (blue arrow, Figure 1B, I). The ability to implant mesh electronics with fully extended structures in targeted brain regions using this methodology was confirmed by micro-computed tomography (micro-CT, Figure 1B, II) and histology.[34] The positioning precision of electrodes in the mesh electronics during the injection process is measured as ca. 20 μm, smaller than the thickness of key subfields and layers within the brain (ca. 60-600 μm, as noted above[45–47]), and thus indicates that the FoV injection method can achieve precise targeted delivery of mesh electronics. In addition, the common use and availability of stereotaxic injection in neuroscience animal research makes this method of delivery straightforward and simple to adopt in other laboratories.

UNIQUE CHRONIC INTERFACE WITH BRAIN TISSUE

Several studies have now demonstrated that the tissue-like properties of mesh electronics yield little or no adverse chronic brain tissue response following injection/implantation of the mesh probes.[30,33] Immunohistological staining of brain tissue after implantation of

common silicon,[17] tungsten[48] and carbon[10] brain probes has established that these probes evoke chronic immune responses at the probe/tissue interface as evidenced by neuron depletion and glial scar formation. Studies indicate that the deleterious chronic immune response is in part due to the mechanical mismatch between the neural tissue and the probe, and together these factors prohibit stable recording and tracking of electrophysiological activities from single neurons over extended time periods.[18,23,28,49–53]

In direct contrast, time-dependent immunohistological studies of brain tissue containing implanted tissue-like mesh electronics have demonstrated tissue healing without evidence for a chronic immune response (Figure 2).[15,30,33,35] Confocal fluorescence images of probe-containing brain slices at 2 weeks, 4 weeks and 3 months (Figure 2A–C) revealed several unique features. First, the mesh electronics produced little inflammation at short times (2 weeks) post-implantation, evidenced by only a slight accumulation of astrocytes and microglia signals near the mesh boundary, while there was essentially no evidence for a chronic immune response at longer times. Second, images showed that axons and neuron somata started penetrating into the interior of the open mesh electronics at the earliest 2 week time point, and that by 3 months post-injection, there was seamless integration of implanted electronic network and tissue. Third, quantitative immunohistology analyses demonstrated that neuron axons and somata, as well as non-neuronal cells such as astrocytes and microglia, exhibited endogenous distributions from inside to far away from the mesh probe (Figure 2D–F). Taken together, these results have shown that, by addressing key structural, mechanical and topological constraints with our tissue-like mesh electronics, it has been possible to realize a probe that minimizes perturbation of the brain tissue we seek to study, in contrast to commonly used electrophysiology tools. This has not only allowed unique measurements that will be described in the following sections, but also opens up the unique opportunity to exploit biochemical functionalization of mesh electronics for modulating interactions within the brain, as will be discussed at the end of this Perspective.

MESH ELECTRONICS STABLY MONITORS BRAIN ACTIVITY AT THE SINGLE-NEURON LEVEL

The stable and seamless chronic integration of axons and neuron somata throughout the implanted mesh electronics probes has enabled stable measurements of neural activity without influence from chronic gliosis present with other probes. In general, information processing in the brain is carried out by transduction of electrical signals within neurons and transport of neurotransmitters between neurons. Rapid intracellular depolarization and axonal propagation of the action potential in the pre-synaptic neurons result in vesicle-mediated release of neurotransmitters, such as dopamine or γ-aminobutyric acid (GABA), which reach the post-synaptic neuron by diffusion across the synaptic cleft. This then elicits a functional response in the post-synaptic neuron and allows for downstream signal propagation.[1] Electrophysiology of neurons manifests from continuous interrogation of changes in intracellular or local extracellular potentials, which occur as a direct result of these electrical and chemical signals.[54] Due to the technical challenges of *in vivo* intracellular patch clamp that is only applicable to acute recordings in anesthetized animals,[55,56] most intracerebral electrophysiology studies employ single-neuron level extracellular

monitoring of neuronal activity with a focus on improving chronic stability[33] and increasing the throughput of simultaneously measured neurons.[7,32]

A critical challenge for multiplexed *in vivo* brain mapping with mesh electronics has centered on creating structures that can be readily connected to and disconnected from measurement electronics. It is important that the I/O pads corresponding to each electrode remain separate when being connected to an external recording interface, otherwise the crossed wires may short circuit and confound data collection; however, the syringe-injection process makes it topologically difficult to achieve prebonding of I/O pads to a connector. We first solved this challenge with an automated conductive ink printing method,[34] and subsequently, with a more user-friendly plug-and-play I/O interface.[31] The plug-and-play interface, which allows for direct clamping of the mesh electronics I/O pads into a standard zero-insertion force (ZIF) connector, was implemented by redesigning the region of the mesh external to skull. The recording region of the mesh probe is kept identical to previous designs (Figure 3A, green inset) to maintain its tissue-like properties, while the external region consists of a leaf-like stem with parallel interconnects terminating in an array of perpendicularly-oriented input/output (I/O) pads (Figure 3A, blue inset). The width and pitch of the I/O pad array were designed to ensure 100% channel connectivity with blind insertion into the ZIF connector.[31] The external region with I/O pads is injected onto a thin polymer film that allows direct 'by-hand' insertion and clamping of the I/O pads into a ZIF connector pre-mounted on a printed circuit board (PCB, Figure 3B). The PCB is fixed onto the animal's skull as a compact and low mass interface (1.3 g and 0.65 g, with and without the detachable amplifier connected, respectively,[32] compared to at least 3 g for Michigan array silicon probes[7,57]) for removable attachment of measurement electronics during chronic recording from awake restrained or free-moving animals (Figure 3C). In addition to facilitating adoption of the mesh electronics by nonexpert laboratories, the plug-and-play interface has also enabled implementation of sterilization protocols necessary for human surgical environments.

Representative chronic recording data from a 32-channel channel mesh probe highlight several key points about measurements with mesh electronics in live rodent brains. First, as demonstrated in previous immunohistology studies, the implanted mesh electronics probe allows the recording electrodes to detect extracellular action potential firing from an endogenous distribution of neurons in the vicinity of the probe (Figure 4A, I). Second, the recorded traces from the 32 recording electrodes that are distributed at different locations spanning the motor cortex exhibit distinct firing patterns (Figure 4A, II, left) with clear firing events represented by 'spikes', or extracellular action potential waveforms in the magnified time traces (Figure 4A, II, right). Since the appearance of each spike indicates the firing event from a single neuron, such recordings are usually also referred to as 'single-neuron' or 'single-unit' recordings. Third, it is possible for spikes from multiple neurons to be detected simultaneous by the same electrode; however, spikes with origins from different neurons usually display and can be resolved by their distinct waveforms due to differences in relative locations and distances from the same recording electrode.[54] This fact brings immense advantages to processing the single-unit recording data, as it becomes much more computationally efficient to extract all spikes by standard spike sorting algorithms, and perform principal component analysis (PCA) to cluster spikes and assign them to different

putative neurons based on the differences in waveform. An overlay of sorted and clustered spikes for 8 representative channels from the 32-channel multiplexed recordings demonstrates the detection of 1-2 neurons per electrode (Figure 4A, III).

Using the same approach to process the single-unit recording data, chronic recordings obtained from 4 separate, 32-channel mesh probes implanted into the motor cortex and hippocampus in the right and left hemispheres of a mouse at 2 and 4 months (Figure 4B) highlight the unique stability and capabilities of tissue-like mesh electronics.[32] For example, single-unit firing activity was detected in roughly 85% of the 128 channels, and the detected activity in each channel generally remained consistent over the 4-month period of the measurements. For example, ca. 80% of all channels with recorded spikes showed <20% variation in average spike amplitude, and >90% of detected single units at 2 months remained detectable with aforementioned small changes in amplitude at 4 months. These results contrast data reported from conventional microwire electrodes[58] and silicon-based Utah array probes,[25] where the majority of channels exhibit >50% variation in spike amplitude and loss of more than half of initially detected single units after only 1-month post-implantation. Thus, the tissue-like mesh electronics provides a substantial jump forward in capabilities for highly stable and scalable multiplexed chronic recording from the single neuron level upwards.

Highly-stable and multiplexed recording probes will be critical for elucidating mechanisms of neural circuit evolution over months to year-long time spans important in, for example, natural and pathological aging.[59] Indeed, we have carried out recording studies with implanted mesh electronics over nearly a year time-scale where we showed the capability to stably track and record from the same individual neurons for the first time (Figure 4C).[33] For example, PCA of single-unit activity from individual channels (Figure 4C, I) and firing rate analyses from PCA-identified individual neurons (Figure 4C, II) demonstrated stable neuron spiking waveforms and intrinsic biophysical properties (i.e., action potential firing rates)[60] over an 8 month period without behavioral training. Interestingly, extending these studies past the time, 48 weeks, where aging-related changes are observed in mice, chronic recordings with mesh electronics revealed distinct changes in individual neurons (Figure 4C, III). Since no observable changes were found in electrode impedance or cell populations at the mesh probe surface, the neuron-dependent declines in firing rate can be attributed to biologically intrinsic changes in neuronal and neural circuit properties during aging. The unique capability of mesh electronic to stably monitor brain activity at the single-neuron level over months to years opens up unprecedented opportunities for high-resolution, longitudinal studies to interrogate age-dependent neural circuit evolution underlying neurodegenerative processes, such as the memory decline and learning impairment associated with Alzheimer’s disease, from a single-neuron perspective.

MESH ELECTRONICS CHRONICALLY MODULATES BRAIN ACTIVITY WITH STABLE SINGLE-NEURON RESPONSES

Electrophysiology probes can also be used to modulate brain activity by injection of charge above a threshold determined by neuromodulatory efficacy for stimulation or inhibition of

activity.[18,61] While direct electrical modulation serves as the basis for research and therapeutic devices, such as deep brain stimulators used to treat Parkinson's disease,[62,63] the issue of mismatches in structural and physical properties that lead to glial scar formation and micromotion discussed earlier also limit the stability of research probes and medical implants.[64]

In this context, implantation of tissue-like mesh electronics incorporating both stimulation and recording electrodes into brains (Figure 5A) allows for single-neuron level modulation and recording in a natural tissue environment. Simultaneous stimulation and recording studies showed significantly increased firing rates from neurons adjacent to stimulation electrodes as evidenced by reproducible evoked spike trains in repeated stimulation trials (Figure 5B). Moreover, consistent patterns of post-stimulus firing rate modulation from 4 to 14 weeks post-injection of mesh electronics along with spike sorting and PCA analyses confirmed stable single-neuron responses to chronic electrical stimulation over this time period (Figure 5C). The detection of a new neuron at 14 weeks (blue, Figure 5C), which can be attributed to the long-term changes of the local neural circuits as a result of chronic modulation, represents a unique opportunity for future studies. For example, the demonstrated chronic stability of tissue-like mesh electronics with simultaneous modulation and recording could be used to probe causality in neural networks in the absence of deleterious 'probe-induced' cell and tissue changes.

FUTURE DIRECTIONS AND OUTLOOK

The unique characteristics of syringe-injectable mesh electronics as a tissue-like neural probe could enable unprecedented future studies and provide new insight into a variety of biological phenomena in neuroscience and neurology. In particular, many experiments can benefit from the simple, minimally invasive delivery to targeted brain regions, the ability to modify the probe surface with biochemically active molecules, and their long-term biochemical stability that allows them to chronically monitor and modulate electrophysiological and chemical processes in the brain with single-neuron resolution. Below we highlight several general directions for mesh electronics and how they could be used to probe the endogenous biochemical interactions and signaling in a 'natural' brain environment (Figure 6).

The first example we consider comes from recognizing the inability of implanted electrophysiological probes to target and record from specific cell types or neuron subtypes versus the capability to target and optically-image or stimulate specific neuron subtype activity using genetically encoded calcium and voltage indicators[65] or optogenetics,[66] respectively. The natural distribution of both neurons and glial cells achieved post-implantation with tissue-like mesh electronics suggests that functionalization of recording and/or stimulation devices with antibodies or aptamers capable of recognizing and targeting specific cell surface receptors could enable *in vivo* neuron subtype electrophysiology (Figure 6A). We believe the development of such capabilities could open-up broad new opportunities for electrophysiology tools, such as deconstruction of complex neural circuitry based on selective recording from specific subgroups of neurons. Additional, this capability could enable more efficacious electrotherapeutic treatment of neurological diseases such as

Parkinson's disease. We envisage that functionalized electrodes in mesh electronics could selectively target and stimulate medium spiny neurons (MSNs) expressing dopamine type-1 (D1) receptors versus D2 receptors, which are structurally and functionally intertwined to facilitate and inhibit movements via direct and indirect pathways, respectively.[67] By selective inhibitory stimulation of D2 MSNs in the 'motor-inhibiting' indirect pathway, mesh electronics could restore the normal motor functions in Parkinsonian patients with much lower therapeutic threshold and long-term safety and efficacy.[67,68]

In a similar vein, our previous *in vitro* studies using functionalized nanowire FETs for biochemical sensing[36,69,70] and subcellular-resolution electrophysiological recording[38,43] could open up completely new opportunities for mesh electronics in the future. For example, receptor-functionalized nanowire FETs incorporated into mesh electronics could be used for highly-localized, non-destructive detection of neurotransmitters *in vivo*.[41,71,72] Furthermore, nanowire FET devices functionalized with phospholipids[38,43,73] or cell penetrating peptides[74] could enable *in vivo* intracellular recording of multiple neurons simultaneously. Such technology would open substantial new opportunities for understanding and influencing brain activity by providing a direct intracellular interface in live animals.[72,75–77]

We believe that implanted mesh electronics also holds substantial potential for regenerative medicine. The underlying motivation of this direction builds upon the use of earlier mesh electronics as an 'active' engineered neural tissue scaffold[40] and observations that mesh electronics, when injected into the lateral ventricle of a live mouse acted as a scaffold to guide the migration of neural cells.[15] Our more recent histological studies showing the interpenetration of neuron axons and somata into the interior of mesh electronics at days to weeks post-injection[30,33] calls for further investigations to elucidate the relative contributions of tissue remodeling, neurite growth, and migration and development of neural progenitor cells (NPCs). Surface modification of mesh electronics with functional biomolecules known to interact with NPCs and facilitate migration[78] or differentiation[79] could be employed to improve the therapeutic capability of mesh electronics (Figure 6B). By understanding and exploiting the extracellular matrix (ECM)-like properties of mesh electronics to favor migration and development of NPCs from the subventricular and subgranular zones,[80] while simultaneously monitoring and possibly modulating neural activity and circuit connectivity, we envision the potential of targeted injection of mesh electronics to connect endogenous sources of NPCs to regions of damaged tissue for neural tissue repair.

Acknowledgments

We thank the members of the Lieber lab for helpful discussions.

Funding

This work was funded by the Air Force Office of Scientific Research (FA9550-14-1-0136), a Harvard University Physical Sciences and Engineering Accelerator award, the National Institute on Drug Abuse of the National Institutes of Health (1R21DA043985-01), and a National Institutes of Health Director's Pioneer Award (1DP1EB025835-01). G.H. is supported by the Pathway to Independence Award (Parent K99/R00) from the National Institute on Aging of the National Institutes of Health (1K99AG056636-01).

References

1. Kandel, ER., Schwartz, JH., Jessell, TM., Siegelbaum, SA., Hudspeth, AJ. Principles of neural scienceMcGraw-hill; New York: 2013
2. Adrian, ED. The basis of sensation: the action of the sense organsChristophers; London, 22 Berners Steeet, W. 1: 1928
3. Gasser HS, Erlanger J. A study of the action currents of nerve with the cathode ray oscillograph. Am J Physiol. 1922; 62:496–524.
4. Yuste R. From the neuron doctrine to neural networks. Nat Rev Neurosci. 2015; 16:487–497. [PubMed: 26152865]
5. Glickstein, M. Neuroscience: a historical introductionMIT Press; 2014
6. Berenyi A, Somogyvari Z, Nagy AJ, Roux L, Long JD, Fujisawa S, Stark E, Leonardo A, Harris TD, Buzsaki G. Large-scale, high-density (up to 512 channels) recording of local circuits in behaving animals. J Neurophysiol. 2014; 111:1132–1149. [PubMed: 24353300]
7. Jun JJ, Steinmetz NA, Siegle JH, Denman DJ, Bauza M, Barbarits B, Lee AK, Anastassiou CA, Andrei A, Aydin C, Barbic M, Blanche TJ, Bonin V, Couto J, Dutta B, Gratiy SL, Gutnisky DA, Hausser M, Karsh B, Ledochowitsch P, Lopez CM, Mitelut C, Musa S, Okun M, Pachitariu M, Putzeys J, Rich PD, Rossant C, Sun WL, Svoboda K, Carandini M, Harris KD, Koch C, O'Keefe J, Harris TD. Fully integrated silicon probes for high-density recording of neural activity. Nature. 2017; 551:232–236. [PubMed: 29120427]
8. Shobe JL, Claar LD, Parhami S, Bakhurin KI, Masmanidis SC. Brain activity mapping at multiple scales with silicon microprobes containing 1,024 electrodes. J Neurophysiol. 2015; 114:2043–2052. [PubMed: 26133801]
9. Schwarz DA, Lebedev MA, Hanson TL, Dimitrov DF, Lehew G, Meloy J, Rajangam S, Subramanian V, Ifft PJ, Li Z, Ramakrishnan A, Tate A, Zhuang KZ, Nicolelis MAL. Chronic, wireless recordings of large-scale brain activity in freely moving rhesus monkeys. Nat Methods. 2014; 11:670–676. [PubMed: 24776634]
10. Kozai TDY, Langhals NB, Patel PR, Deng XP, Zhang HN, Smith KL, Lahann J, Kotov NA, Kipke DR. Ultrasmall implantable composite microelectrodes with bioactive surfaces for chronic neural interfaces. Nat Mater. 2012; 11:1065–1073. [PubMed: 23142839]
11. Guitchounts G, Markowitz JE, Liberti WA, Gardner TJ. A carbon-fiber electrode array for long-term neural recording. J Neural Eng. 2013; 10:046016. [PubMed: 23860226]
12. Tyler WJ. OPINION The mechanobiology of brain function. Nat Rev Neurosci. 2012; 13:867–878. [PubMed: 23165263]
13. Steif, PS. Mechanics of materialsPearson; Upper Saddle River, NJ: 2012
14. Lee H, Bellamkonda RV, Sun W, Levenston ME. Biomechanical analysis of silicon microelectrode-induced strain in the brain. J Neural Eng. 2005; 2:81–89. [PubMed: 16317231]
15. Liu J, Fu TM, Cheng ZG, Hong GS, Zhou T, Jin LH, Duvvuri M, Jiang Z, Kruskal P, Xie C, Suo ZG, Fang Y, Lieber CM. Syringe-injectable electronics. Nat Nanotechnol. 2015; 10:629–636. [PubMed: 26053995]
16. Rousche PJ, Pellinen DS, Pivin DP, Williams JC, Vetter RJ, Kipke DR. Flexible polyimide-based intracortical electrode arrays with bioactive capability. IEEE Trans Biomed Eng. 2001; 48:361–371. [PubMed: 11327505]
17. Biran R, Martin DC, Tresco PA. Neuronal cell loss accompanies the brain tissue response to chronically implanted silicon microelectrode arrays. Exp Neurol. 2005; 195:115–126. [PubMed: 16045910]
18. Chen R, Canales A, Anikeeva P. Neural recording and modulation technologies. Nat Rev Mater. 2017; 2:16093.
19. Kasthuri N, Hayworth KJ, Berger DR, Schalek RL, Conchello JA, Knowles-Barley S, Lee D, Vazquez-Reina A, Kaynig V, Jones TR, Roberts M, Morgan JL, Tapia JC, Seung HS, Roncal WG, Vogelstein JT, Burns R, Sussman DL, Priebe CE, Pfister H, Lichtman JW. Saturated Reconstruction of a Volume of Neocortex. Cell. 2015; 162:648–661. [PubMed: 26232230]
20. Eroglu C, Barres BA. Regulation of synaptic connectivity by glia. Nature. 2010; 468:223–231. [PubMed: 21068831]

21. Clarke LE, Barres BA. Emerging roles of astrocytes in neural circuit development. Nat Rev Neurosci. 2013; 14:311–321. [PubMed: 23595014]
22. Saxena T, Bellamkonda RV. Implantable electronics: A sensor web for neurons. Nat Mater. 2015; 14:1190–1191. [PubMed: 26585085]
23. Polikov VS, Tresco PA, Reichert WM. Response of brain tissue to chronically implanted neural electrodes. J Neurosci Meth. 2005; 148:1–18.
24. Perge JA, Homer ML, Malik WQ, Cash S, Eskandar E, Friehs G, Donoghue JP, Hochberg LR. Intra-day signal instabilities affect decoding performance in an intracortical neural interface system. J Neural Eng. 2013; 10:036004. [PubMed: 23574741]
25. Dickey AS, Suminski A, Amit Y, Hatsopoulos NG. Single-Unit Stability Using Chronically Implanted Multielectrode Arrays. J Neurophysiol. 2009; 102:1331–1339. [PubMed: 19535480]
26. Jackson A, Fetz EE. Compact movable microwire array for long-term chronic unit recording in cerebral cortex of primates. J Neurophysiol. 2007; 98:3109–3118. [PubMed: 17855584]
27. Aflalo T, Kellis S, Klaes C, Lee B, Shi Y, Pejsa K, Shanfield K, Hayes-Jackson S, Aisen M, Heck C, Liu C, Andersen RA. Decoding motor imagery from the posterior parietal cortex of a tetraplegic human. Science. 2015; 348:906–910. [PubMed: 25999506]
28. Bensmaia SJ, Miller LE. Restoring sensorimotor function through intracortical interfaces: progress and looming challenges. Nat Rev Neurosci. 2014; 15:313–325. [PubMed: 24739786]
29. Hong G, Yang X, Zhou T, Lieber CM. Mesh electronics: a new paradigm for tissue-like brain probes. Curr Opin Neurobiol. 2018; 50:33–41. [PubMed: 29202327]
30. Zhou T, Hong G, Fu TM, Yang X, Schuhmann TG, Viveros RD, Lieber CM. Syringe-injectable mesh electronics integrate seamlessly with minimal chronic immune response in the brain. Proc Natl Acad Sci USA. 2017; 114:5894–5899. [PubMed: 28533392]
31. Schuhmann TG, Yao J, Hong G, Fu TM, Lieber CM. Syringe-Injectable Electronics with a Plug-and-Play Input/Output Interface. Nano Lett. 2017; 17:5836–5842. [PubMed: 28787578]
32. Fu TM, Hong G, Viveros RD, Zhou T, Lieber CM. Highly scalable multichannel mesh electronics for stable chronic brain electrophysiology. Proc Natl Acad Sci USA. 2017; 114:E10046–E10055. [PubMed: 29109247]
33. Fu TM, Hong GS, Zhou T, Schuhmann TG, Viveros RD, Lieber CM. Stable long-term chronic brain mapping at the single-neuron level. Nat Methods. 2016; 13:875–882. [PubMed: 27571550]
34. Hong GS, Fu TM, Zhou T, Schuhmann TG, Huang JL, Lieber CM. Syringe Injectable Electronics: Precise Targeted Delivery with Quantitative Input/Output Connectivity. Nano Lett. 2015; 15:6979–6984. [PubMed: 26317328]
35. Xie C, Liu J, Fu TM, Dai XC, Zhou W, Lieber CM. Three-dimensional macroporous nanoelectronic networks as minimally invasive brain probes. Nat Mater. 2015; 14:1286–1292. [PubMed: 26436341]
36. Cui Y, Wei QQ, Park HK, Lieber CM. Nanowire nanosensors for highly sensitive and selective detection of biological and chemical species. Science. 2001; 293:1289–1292. [PubMed: 11509722]
37. Patolsky F, Timko BP, Yu GH, Fang Y, Greytak AB, Zheng GF, Lieber CM. Detection, stimulation, and inhibition of neuronal signals with high-density nanowire transistor arrays. Science. 2006; 313:1100–1104. [PubMed: 16931757]
38. Tian BZ, Cohen-Karni T, Qing Q, Duan XJ, Xie P, Lieber CM. Three-Dimensional, Flexible Nanoscale Field-Effect Transistors as Localized Bioprobes. Science. 2010; 329:830–834. [PubMed: 20705858]
39. Lieber, CM. Nano/Bio Interface Center (NBIC) Award for Research Excellence in Nanotechnology SpeechUniversity of Pennsylvania; Oct, 2007 Nanotechnology and the Life Sciences.
40. Tian BZ, Liu J, Dvir T, Jin LH, Tsui JH, Qing Q, Suo ZG, Langer R, Kohane DS, Lieber CM. Macroporous nanowire nanoelectronic scaffolds for synthetic tissues. Nat Mater. 2012; 11:986–994. [PubMed: 22922448]
41. Zhang AQ, Lieber CM. Nano-Bioelectronics. Chem Rev. 2016; 116:215–257. [PubMed: 26691648]
42. Tian BZ, Lieber CM. Synthetic Nanoelectronic Probes for Biological Cells and Tissues. Annu Rev Anal Chem. 2013; 6:31–51.

43. Qing Q, Jiang Z, Xu L, Gao RX, Mai LQ, Lieber CM. Free-standing kinked nanowire transistor probes for targeted intracellular recording in three dimensions. Nat Nanotechnol. 2014; 9:142–147. [PubMed: 24336402]
44. Dai XC, Zhou W, Gao T, Liu J, Lieber CM. Three-dimensional mapping and regulation of action potential propagation in nanoelectronics-innervated tissues. Nat Nanotechnol. 2016; 11:776–782. [PubMed: 27347837]
45. Lein ES, Hawrylycz MJ, Ao N, Ayres M, Bensinger A, Bernard A, Boe AF, Boguski MS, Brockway KS, Byrnes EJ, Chen L, Chen L, Chen TM, Chin MC, Chong J, Crook BE, Czaplinska A, Dang CN, Datta S, Dee NR, Desaki AL, Desta T, Diep E, Dolbeare TA, Donelan MJ, Dong HW, Dougherty JG, Duncan BJ, Ebbert AJ, Eichele G, Estin LK, Faber C, Facer BA, Fields R, Fischer SR, Fliss TP, Frensley C, Gates SN, Glattfelder KJ, Halverson KR, Hart MR, Hohmann JG, Howell MP, Jeung DP, Johnson RA, Karr PT, Kawal R, Kidney JM, Knapik RH, Kuan CL, Lake JH, Laramee AR, Larsen KD, Lau C, Lemon TA, Liang AJ, Liu Y, Luong LT, Michaels J, Morgan JJ, Morgan RJ, Mortrud MT, Mosqueda NF, Ng LL, Ng R, Orta GJ, Overly CC, Pak TH, Parry SE, Pathak SD, Pearson OC, Puchalski RB, Riley ZL, Rockett HR, Rowland SA, Royall JJ, Ruiz MJ, Sarno NR, Schaffnit K, Shapovalova NV, Sivisay T, Slaughterbeck CR, Smith SC, Smith KA, Smith BI, Sodt AJ, Stewart NN, Stumpf KR, Sunkin SM, Sutram M, Tam A, Teemer CD, Thaller C, Thompson CL, Varnam LR, Visel A, Whitlock RM, Wohnoutka PE, Wolkey CK, Wong VY, Wood M, Yaylaoglu MB, Young RC, Youngstrom BL, Yuan XF, Zhang B, Zwingman TA, Jones AR. Genome-wide atlas of gene expression in the adult mouse brain. Nature. 2007; 445:168–176. [PubMed: 17151600]
46. Hattox AM, Nelson SB. Layer V neurons in mouse cortex projecting to different targets have distinct physiological properties. J Neurophysiol. 2007; 98:3330–3340. [PubMed: 17898147]
47. Buckmaster PS, Wen X, Toyoda I, Gulland FM, Van Bonn W. Hippocampal neuropathology of domoic acid-induced epilepsy in California sea lions (Zalophus californianus). J Comp Neurol. 2014; 522:1691–1706. [PubMed: 24638960]
48. Prasad A, Xue QS, Sankar V, Nishida T, Shaw G, Streit WJ, Sanchez JC. Comprehensive characterization and failure modes of tungsten microwire arrays in chronic neural implants. J Neural Eng. 2012; 9:056015. [PubMed: 23010756]
49. Lacour SP, Courtine G, Guck J. Materials and technologies for soft implantable neuroprostheses. Nat Rev Mater. 2016; 1:16063.
50. Luan L, Wei X, Zhao Z, Siegel JJ, Potnis O, Tuppen CA, Lin S, Kazmi S, Fowler RA, Holloway S, Dunn AK, Chitwood RA, Xie C. Ultraflexible nanoelectronic probes form reliable, glial scar-free neural integration. Sci Adv. 2017; 3:e1601966. [PubMed: 28246640]
51. Rivnay J, Wang HL, Fenno L, Deisseroth K, Malliaras GG. Next-generation probes, particles, and proteins for neural interfacing. Sci Adv. 2017; 3:e1601649. [PubMed: 28630894]
52. Ferro MD, Melosh NA. Electronic and Ionic Materials for Neurointerfaces. Adv Funct Mater. 2018; 28doi: 10.1002/adfm.201704335
53. Salatino JW, Ludwig KA, Kozai TDY, Purcell EK. Glial responses to implanted electrodes in the brain. Nat Biomed Eng. 2017; 1:862–877.
54. Gold C, Henze DA, Koch C, Buzsaki G. On the origin of the extracellular action potential waveform: A modeling study. J Neurophysiol. 2006; 95:3113–3128. [PubMed: 16467426]
55. Arenz A, Silver RA, Schaefer AT, Margrie TW. The contribution of single synapses to sensory representation in vivo. Science. 2008; 321:977–980. [PubMed: 18703744]
56. Kodandaramaiah SB, Holst GL, Wickersham IR, Singer AC, Franzesi GT, McKinnon ML, Forest CR, Boyden ES. Assembly and operation of the autopatcher for automated intracellular neural recording in vivo. Nat Protoc. 2016; 11:634–654. [PubMed: 26938115]
57. Rios G, Lubenov EV, Chi D, Roukes ML, Siapas AG. Nanofabricated Neural Probes for Dense 3-D Recordings of Brain Activity. Nano Lett. 2016; 16:6857–6862. [PubMed: 27766885]
58. Liu X, McCreery DB, Carter RR, Bullara LA, Yuen TG, Agnew WF. Stability of the interface between neural tissue and chronically implanted intracortical microelectrodes. IEEE Trans Rehabil Eng. 1999; 7:315–326. [PubMed: 10498377]
59. Grady C. BRAIN AGEING The cognitive neuroscience of ageing. Nat Rev Neurosci. 2012; 13:491–505. [PubMed: 22714020]

60. Shadlen MN, Newsome WT. The variable discharge of cortical neurons: implications for connectivity, computation, and information coding. J Neurosci. 1998; 18:3870–3896. [PubMed: 9570816]
61. Cogan SF. Neural stimulation and recording electrodes. Annu Rev Biomed Eng. 2008; 10:275–309. [PubMed: 18429704]
62. Kringelbach ML, Jenkinson N, Owen SLF, Aziz TZ. Translational principles of deep brain stimulation. Nat Rev Neurosci. 2007; 8:623–635. [PubMed: 17637800]
63. Fasano A, Aquino CC, Krauss JK, Honey CR, Bloem BR. Axial disability and deep brain stimulation in patients with Parkinson disease. Nat Rev Neurol. 2015; 11:98–110. [PubMed: 25582445]
64. Cicchetti F, Barker RA. The glial response to intracerebrally delivered therapies for neurodegenerative disorders: is this a critical issue? Front Pharmacol. 2014; 5:139. [PubMed: 25071571]
65. Lin MZ, Schnitzer MJ. Genetically encoded indicators of neuronal activity. Nat Neurosci. 2016; 19:1142–1153. [PubMed: 27571193]
66. Deisseroth K. Optogenetics: 10 years of microbial opsins in neuroscience. Nat Neurosci. 2015; 18:1213–1225. [PubMed: 26308982]
67. Calabresi P, Picconi B, Tozzi A, Ghiglieri V, Di Filippo M. Direct and indirect pathways of basal ganglia: a critical reappraisal. Nat Neurosci. 2014; 17:1022–1030. [PubMed: 25065439]
68. Kravitz AV, Freeze BS, Parker PRL, Kay K, Thwin MT, Deisseroth K, Kreitzer AC. Regulation of parkinsonian motor behaviours by optogenetic control of basal ganglia circuitry. Nature. 2010; 466:622–626. [PubMed: 20613723]
69. Zheng GF, Patolsky F, Cui Y, Wang WU, Lieber CM. Multiplexed electrical detection of cancer markers with nanowire sensor arrays. Nat Biotechnol. 2005; 23:1294–1301. [PubMed: 16170313]
70. Gao N, Zhou W, Jiang X, Hong G, Fu TM, Lieber CM. General strategy for biodetection in high ionic strength solutions using transistor-based nanoelectronic sensors. Nano Lett. 2015; 15:2143–2148. [PubMed: 25664395]
71. Fu TM, Duan XJ, Jiang Z, Dai XC, Xie P, Cheng ZG, Lieber CM. Sub-10-nm intracellular bioelectronic probes from nanowire-nanotube heterostructures. Proc Natl Acad Sci USA. 2014; 111:1259–1264. [PubMed: 24474745]
72. Kruskal PB, Jiang Z, Gao T, Lieber CM. Beyond the Patch Clamp: Nanotechnologies for Intracellular Recording. Neuron. 2015; 86:21–24. [PubMed: 25856481]
73. Almquist BD, Melosh NA. Fusion of biomimetic stealth probes into lipid bilayer cores. Proc Natl Acad Sci USA. 2010; 107:5815–5820. [PubMed: 20212151]
74. Lee JH, Zhang AQ, You SS, Lieber CM. Spontaneous Internalization of Cell Penetrating Peptide-Modified Nanowires into Primary Neurons. Nano Lett. 2016; 16:1509–1513. [PubMed: 26745653]
75. Bean BP. The action potential in mammalian central neurons. Nat Rev Neurosci. 2007; 8:451–465. [PubMed: 17514198]
76. Long MA, Lee AK. Intracellular recording in behaving animals. Curr Opin Neurobiol. 2012; 22:34–44. [PubMed: 22054814]
77. Angle MR, Cui BX, Melosh NA. Nanotechnology and neurophysiology. Curr Opin Neurobiol. 2015; 32:132–140. [PubMed: 25889532]
78. Whalley K. STEM CELLS At home with neural stem cells. Nat Rev Neurosci. 2008; 9:801–801.
79. Gao J, Kim YM, Coe H, Zern B, Sheppard B, Wang Y. A neuroinductive biomaterial based on dopamine. Proc Natl Acad Sci USA. 2006; 103:16681–16686. [PubMed: 17075054]
80. Ghashghaei HT, Lai C, Anton ES. Neuronal migration in the adult brain: are we there yet? Nat Rev Neurosci. 2007; 8:141–151. [PubMed: 17237805]

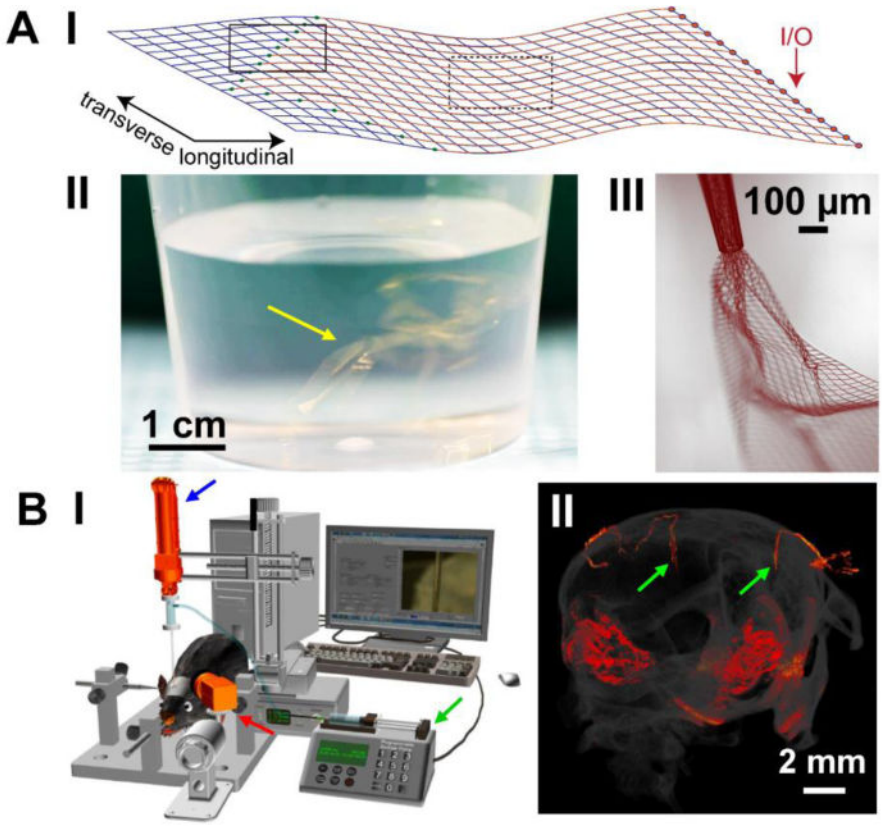

Figure 1.

Design and delivery of mesh electronics probes. (A) Unique structural and mechanical design of mesh electronics enables novel syringe-assisted delivery through a needle. I, Schematic of 16-channel mesh electronics, highlighting the recording electrodes (green dots in solid black box), metal interconnects (red lines in dashed black box) and I/O pads (red arrow). II, Photograph of a beaker with multiple 16-channel mesh electronics probes (yellow arrow) suspended in an aqueous saline solution; the golden color corresponds to light scattered and reflected from 10 μm wide, 100 nm thick metal interconnect lines. III, Bright-field microscope image taken in wide-field transmission mode showing partially ejected mesh electronics through a glass needle with an I.D. of 95 μm, exhibiting significant expansion and unfolding of mesh electronics in aqueous solution. (B) Controlled stereotaxic injection allows precisely targeted delivery of mesh electronics in the brain. I, Schematic of the semi-automated instrumentation for controlled injection of mesh electronics, highlighting a syringe pump for controlling the volumetric injection rate (green arrow), the motorized translation stage for controlling needle withdrawal (blue arrow), and the CCD camera for visualizing the mesh in the FoV (red arrow). II, Micro-CT image showing two fully extended mesh electronics probes (red linear structures highlighted by green arrows) within the brain following controlled injection. The other reddish areas correspond to the skull and mesh probe (I/O region) on the outer surface of the skull. Reproduced with permission from refs. [15] and [34].

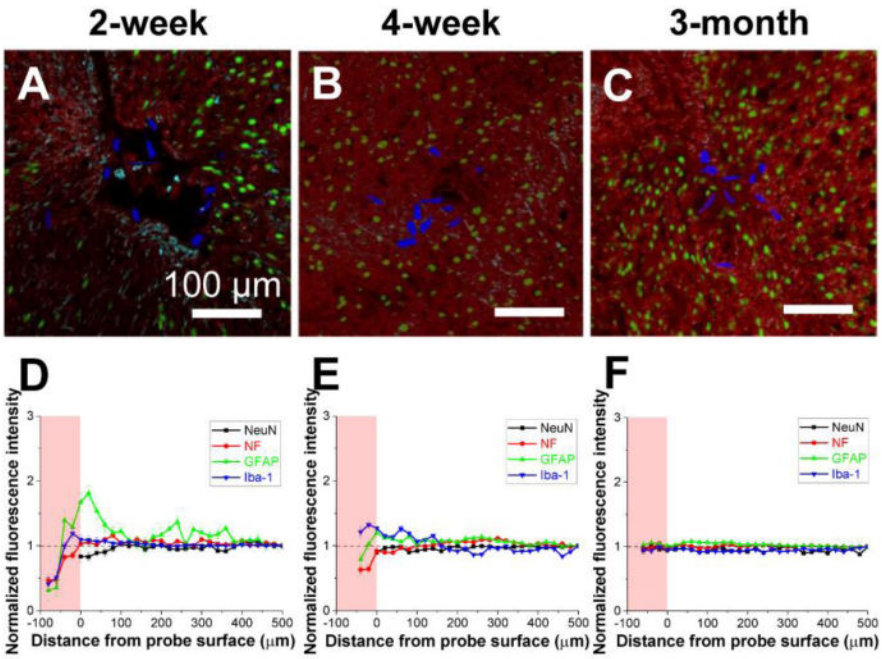

Figure 2.

Time-dependent histology of the mesh electronics/brain tissue interface. (A-C) Confocal fluorescence microscopy images of 10-μm thick horizontal brain slices sectioned perpendicular to the long axis of mesh probes at (A) 2, (B) 4 and (C) 12 weeks post-injection. Green, red, cyan and blue colors correspond to neuron nuclei (NeuN antibody), neuron axons (neurofilament antibody), astrocytes (glial fibrillary acidic protein, GFAP antibody) and mesh electronics, respectively. (D-F) Normalized fluorescence intensity plotted as a function of distance from the boundary of mesh electronics at (D) 2, (E) 4 and (F) 12 weeks post-injection. The pink shaded regions indicate the interior of the mesh electronics, and the error bars represent the standard error of the mean (s.e.m.). Reproduced with permission from ref. 30.

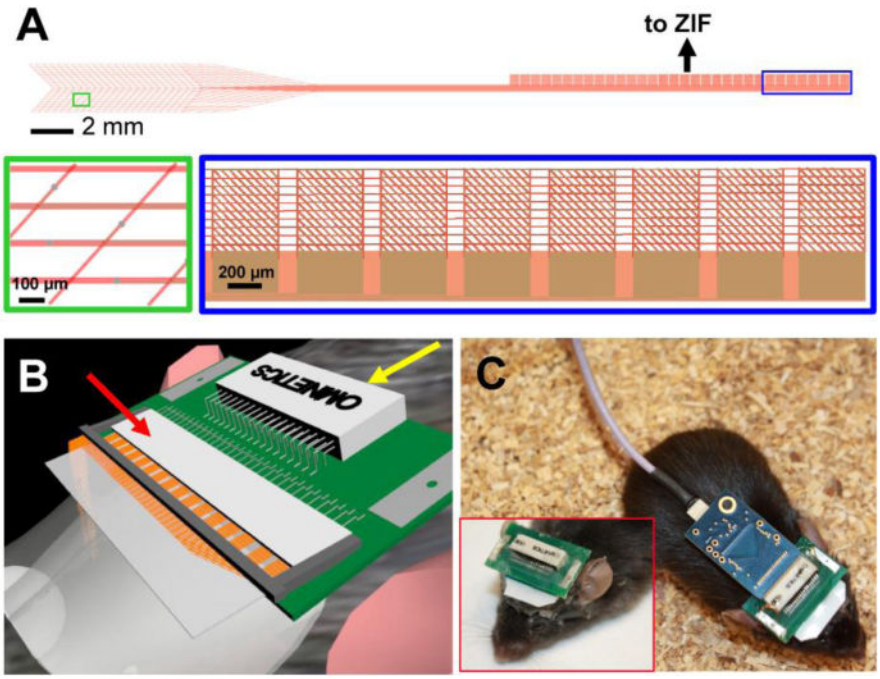

Figure 3.

Syringe-injectable mesh electronics with plug-and-play interface. (A) Schematic diagram of the plug-and-play mesh electronics, where the ultraflexible recording region (green box; lower left inset, zoom) converges to a flexible stem terminating in mesh metal I/O pads perpendicular to the stem (blue box; lower right inset, zoom). The stem and mesh I/O remain outside the skull. (B) Schematic diagram of direct clamping of the mesh I/O pads into a PCB-mounted ZIF connector (red arrow), which can then be connected to measurement electronics via a standard Omnetics connector (yellow arrow) mounted on the same PCB. (C) Photograph showing electrophysiological recording of a freely moving mouse injected with mesh electronics; the inset shows the part of the interface that remains permanently attached to the mouse head without the amplifier and the cable connected. Reproduced with permission from refs. [29] and [31].

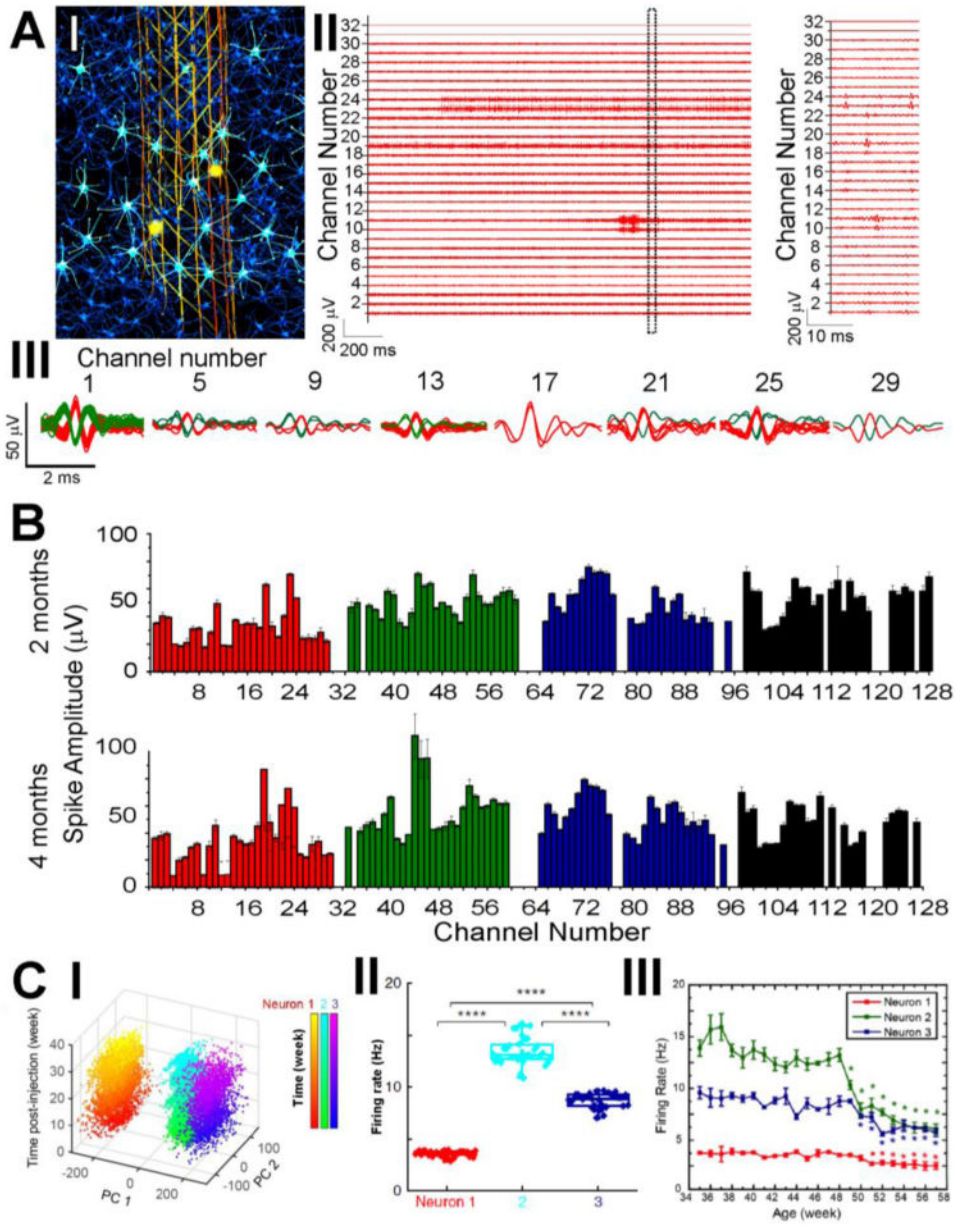

Figure 4.

Highly multiplexed, chronically stable *in vivo* electrophysiology in mice. (A) Electrophysiological recording of single-neuron action potentials in mouse brain. I, Schematic of *in vivo* recording of neuron activities via the seamless integrated interface between the injected mesh electronics and the endogenous neural tissue. Electrically active neurons are highlighted in bright cyan color, with their firing activities detected by a subset of recording electrodes (yellow circles) in the mesh electronics at a time. II, Representative multiplexed extracellular single-neuron recording traces from a 32-channel mesh electronics probe at 2 months post-injection into the mouse motor cortex, with a magnified view of a 20-ms segment highlighting the waveforms of detected single-unit action potentials in Channels 10, 11, 19, 23 and 24. III, Overlay of sorted and clustered spikes from a subset of

selected channels by processing the raw data of recording traces shown in A, II. Red and green colors are used to denote spikes assigned to different neurons. (B) Average single-unit spike amplitudes from simultaneous 128-channel recording in a mouse brain using 4 separate 32-channel mesh electronics probes at 2 and 4 months post-injection. The error bars represent the s.e.m. (C) Time-dependent consistent tracking of the same individual neurons based on single-unit spike recording, sorting and clustering as shown in B. I, PCA-separated clusters of single-unit firing activity are stable over the course of 34 weeks post-injection in young mice. II, PCA-identified neurons from C, I demonstrate stable firing rates across the analyzed 34 weeks. III, Age-dependent individual neuron firing rate changes in middle-aged mice demonstrate systematic decline. Reproduced with permission from refs. [32] and [33].

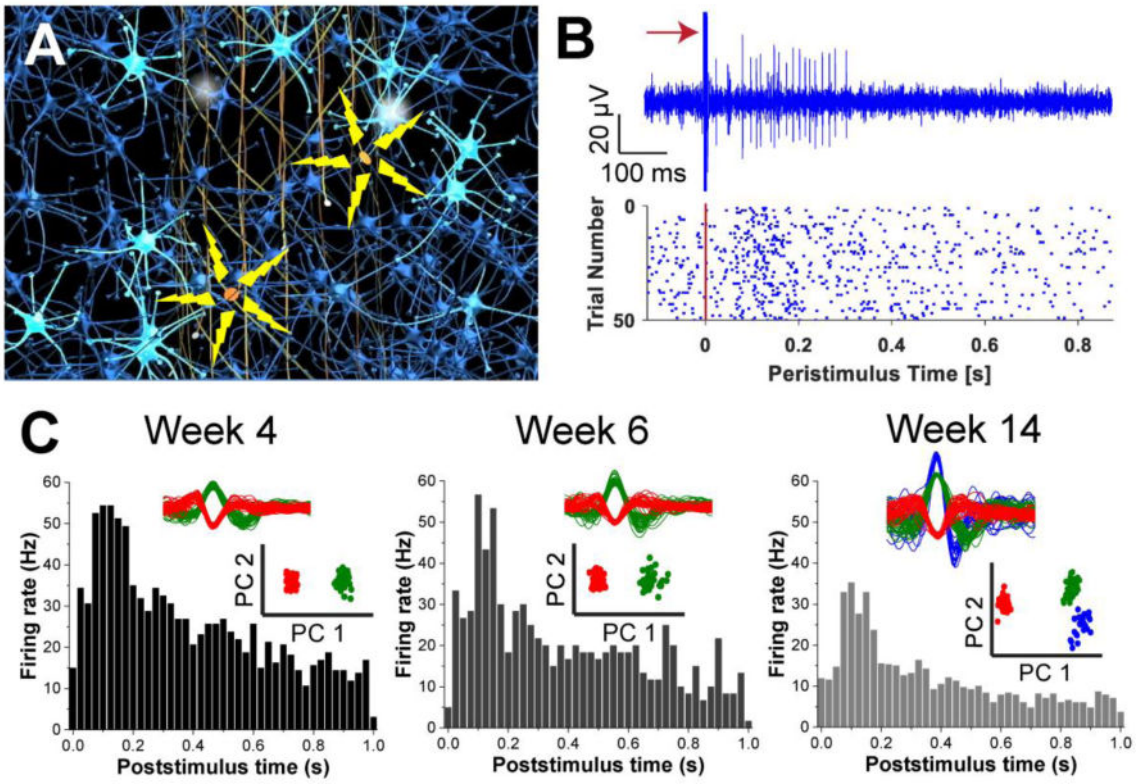

Figure 5.

Precision modulation of neural activity. (A) Schematic of mesh electronics with stimulation & recording electrodes where precise circuit modulation with simultaneous recording is highlighted from two stimulation sites. (B) A representative stimulus-evoked single-unit firing trace with a red arrow indicating the stimulus (top), and a raster plot showing single-unit firing events (blue dots) before and after an electrical stimulus is given (red solid line, t = 0 s) for 50 trials (bottom). (C) Poststimulus time histograms from a representative recording electrode in the vicinity of a stimulation electrode at 4, 6, and 14 weeks post-injection of the mesh probe. Spike-sorting and PCA clustering results with corresponding colors are shown as insets. Reproduced with permission from ref. 33.

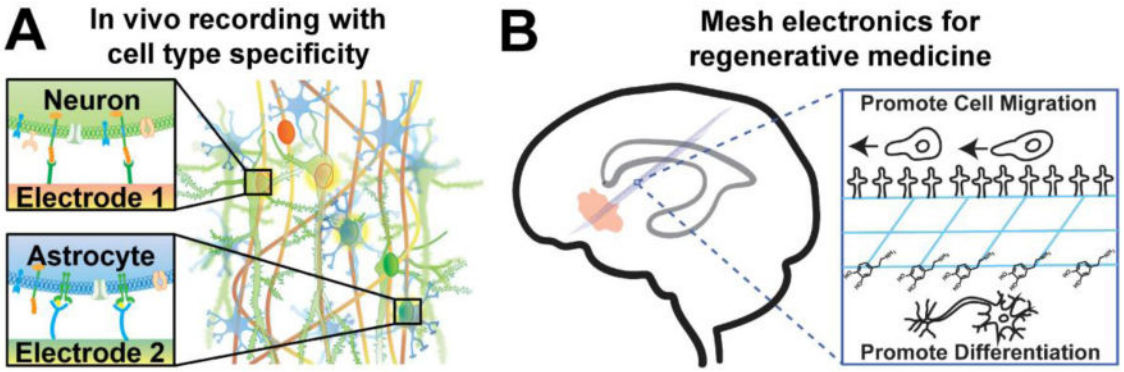

Figure 6.

Future directions for tissue-like mesh electronics. (A) Antibodies or aptamers on electrodes could be used to attract and target specific cell types, allowing selective electrophysiological monitoring of different cell types on different electrodes. (B) Mesh electronics (blue) could be used to connect brain regions containing NPCs (grey) to sites of tissue damage (pink). Biochemical modification of the surfaces of mesh electronics could be used to promote cellular migration towards damage and differentiation to desired cell types near damage while monitoring and/or modulating activity with the integrated electrodes.